Forward Modeling of Ground-penetrating Radar Data for a 2-D Environment

Luiz Rijo

Curso de Pós-graduação em Geofísica, UFPa. Belém, Pará

Abstract

Forward modeling of ground-penetrating radar is developed using a simplistic 2-D algorithm based on the finite element method. To keep the problem fully two-dimensional, a line-source of current is used to simulate the antenna. The finite element computation is done in term of the scattered electric field produced by two-dimensional lateral variation of electric conductivity, dielectric permittivity and magnetic permeability with respect to a background-layered earth. Comparison of normal incident synthetic radargrams for 1-D and 2-D environments with and without losses is analyzed to get insight about the resolution of GPR data.

INTRODUCTION

Ground-Penetrating Radar (GPR) has been applied in a variety of shallow high-resolution geophysical investigations such as: identification of buried hazardous wastes, soil mappings, groundwater studies, archaeology, geo-technical analysis and technical police investigation. Most of the forward GPR modeling has been done with ray-tracing technique borrowed from seismic. Modeling GPR data by solving electromagnetic boundary value problems has been restricted mostly to 1-D structures. The purpose of this paper is to introduce a simple 2-D GPR modeling algorithm based on the finite element method. To keep the problem as simple as possible we use as "antenna" an infinite line-source of electric current parallel to the strike of the 2-D structures (see Schoolmeester et. al., 1995). To simulate the shape of the radar antenna pulse a 500 MHz sinusoidal response having a 3/2 cycle pulse width is used. The problem is solved in frequency and wave number domains and transformed back to space and time domains via FFT.

THE ALGORITHM

At the ground surface, the time-domain electric field $e_y(x, 0, t)$ is given by the Fourier transform of the corresponding

$$e_y(x,0,t) = \frac{1}{2\pi}\int_{-\infty}^{\infty} E_y(x,0,\omega)e^{i\omega t}d\omega. \tag{1}$$

frequency-domain field $E_y(x, 0, \omega)$,

In order to calculate the frequency-domain electric field $E_y(x, 0, \omega)$ it is computationally convenient at the outset to decompose the field in its primary and secondary components. The primary component is associated with the layered earth, denoted background model, and the secondary component is the scattered field produced by two-dimensional lateral heterogeneity hosted within the layered earth. Thus, we can write,

$$E_y(x,0,\omega) = E_y^p(x,0,\omega) + E_y^s(x,0,\omega),$$

in which the primary field is given by (Wait, 1962),

$$E_y^p = \frac{-i\omega\mu_0 I(\omega)}{2\pi}\int_0^{\infty}\frac{1}{u_0}(1+R_0)e^{u_0 h_0}\cos(k_x x)dk_x, \tag{2}$$

where $I(\omega)$ is the spectrum of pulse in the line-source, $R_0 = (u_0 - u_1F_1)/(u_0 + u_1F_1)$ is the *reflection coefficient* at the air-earth interface, $u_0 = (k^2_x - \omega^2\mu_0\varepsilon_0)^{1/2}$ and $u_1 = (k^2_x + i\omega\mu_0(\sigma_1 + i\omega\varepsilon_1)^{1/2}$ are the propagation constants above and just below the ground surface. The *stratification coefficient* F_1 in the expression of the reflection coefficient R_0 is obtained by the recursion formula,

$$F_j = \frac{u_{j+1}F_{j+1} + u_j\tanh(u_j h_j)}{u_j + u_{j+1}F_{j+1}\tanh(u_j h_j)}, \qquad j = 1,2,3,..,N-1, \tag{3}$$

starting with $F_N = 1$ at the lowermost layer (see Figure 1). The term h_0 is the height of the line-source above the surface. The secondary field is given by a boundary value problem involving the Helmholtz equation,

$$\frac{\partial^2 E_y^s}{\partial x^2} + \frac{\partial^2 E_y^s}{\partial z^2} - i\omega\mu_0(\sigma + i\omega\varepsilon)E_y^s = i\omega\mu_0(\Delta\sigma + i\omega\Delta\varepsilon)E_y^p, \tag{4}$$

in which the source term $(\Delta\sigma+i\omega\Delta\varepsilon)E_y^p$ is the density of primary electric current at the positions where the electrical properties (electric conductivity and dielectric permittivity) departure from those of the layered earth. Dirichlet homogeneous boundary condition is imposed at great distance from any lateral variations of electrical properties.
The primary electric field $E_y(x, z. \omega)$ included in the above-mentioned source term is given by

$$E_y^p = \frac{-i\omega\mu_0 I(\omega)}{2\pi}\int_0^\infty \frac{E_j}{u_0}\left[e^{-u_j(z-z_j)} + e^{u_j(z-z_j)}\right]e^{u_0 h_0}\cos(k_x x)dk_x, \qquad (5)$$

where the coefficients E_j of the jth-layer containing the two-dimensional heterogeneity is given by the recursion formula

$$E_j = E_{j-1}\frac{(1+R_j)e^{u_j h_j}}{1+R_j e^{2u_j h_j}}, \qquad j = 1,2,...N-1,$$

$$E_n = E_{N-1}(1+R_{N-1}), \qquad i = 1,2,3,$$

starting with $E_0 = 1$. In the reflection coefficient $R_j = (u_j - u_{j+1}F_{j+1})/(u_j + u_{j+1}F_{j+1})$, the propagation constants are expressed by $u_j = (k^2_x + i\omega\mu_0(\sigma_j + i\omega\varepsilon_j)^{1/2}$ and the stratification coefficients F_{j-1} are obtained by the recursion formula (3).

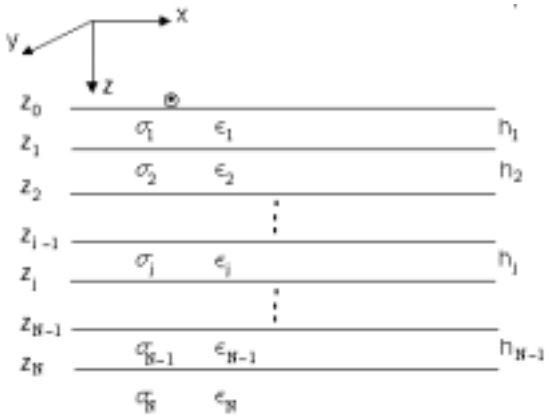

Figure 1. Geometry of the primary or background model.

The Helmholtz equation (4) can not be solved analytically. Thus, we content with numerical solution. We chose the finite element method for its simplicity and flexibility to handle complex models (Strang and Fix, 1972). After dividing the domain (a finite portion of the region where the solution is thought) in small triangles, denoted elements (see Figure 2), this technique consists of using linear basis functions at each element to interpolate the desired solution using the Galerkin variational formulation equivalent to (4).

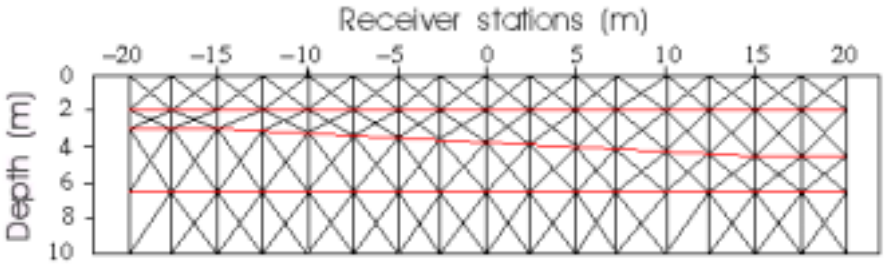

Figure 2. Central portion of the finite-element mesh.

For each triangle Ω^e we may write, after applying the Galerkin's rule, the element matrix and the element source vector as following

$$k_{ij} = \int_{\Omega^e}\left(\frac{\partial\Psi_i}{\partial x}\frac{\partial\Psi_j}{\partial x} + \frac{\partial\Psi_i}{\partial z}\frac{\partial\Psi_j}{\partial z}\right)dxdz + i\omega\mu_0\int_{\Omega^e}(\sigma + i\omega\varepsilon)\Psi_i\Psi_j dxdz, \qquad i,j = 1,2,3,$$

and

$$f_i = -i\omega\mu_0\int_{\Omega^e}(\Delta\sigma + i\omega\Delta\varepsilon)E_y^p\Psi_i dxdz \qquad i = 1,2,3,$$

after using the continuity of the tangential component of the electrical field at the element boundaries. These element matrices and source vectors are assembled to form the global system of linear equations. After incorporating the Dirichlet homogeneous boundary condition at the edge of the domain, the global system of linear equations is solved to given the secondary field at each node of the finite-element grid.
Finally, at the ground surface, this secondary field is added to the primary field (2) to produce the total field at the frequency domain. The radar trace for each line-source position is obtained by inverse Fourier transform using FFT of the total field.

RESULTS

To show the performance of the above-mentioned algorithm we carried out a set of simple experiments. Let us consider the models shown in Figure 3. The model 1-D is simply a three horizontal layer earth with thicknesses equal to 2, 1 and 3.5 meters over an infinitely thick basement. The model 2-D is a variation of model 1-D with the interface between the second and third layers dipping from the left toward the right side. With these two models we performed three experiments varying the electric conductivity and relative dielectric permittivity of the layers accord to Table I.

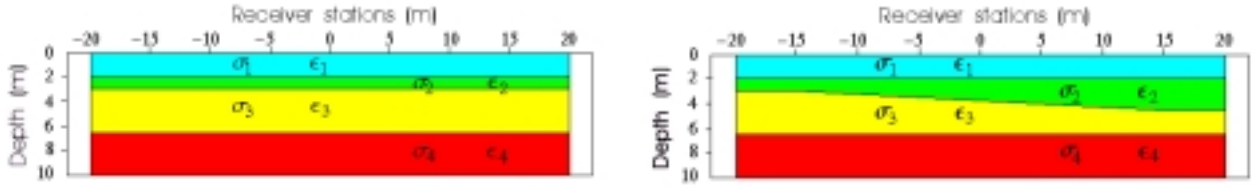

Figure 3 - Model 1D (left) and Model 2D (right) used in the experiments.

TABLE I - Conductivities (siemens/m) and dielectric constants used in the model 1D and 2D.

	σ_1	ε_{r1}	σ_2	ε_{r2}	σ_3	ε_{r3}	σ_4	ε_{r4}
Experiment 1	0	7	0	5	0	10	0	20
Experiment 2	0.001	7	0.002	5	0.01	10	0.005	20
Experiment 3	0.002	7	0.005	5	0.01	10	0.005	20

For the first experiment we made the conductivity of each layer equal to zero. Thus, we neglected the losses. The corresponding zero offset radargrams are shown in Figure 4a and 4b. For both models, we clearly observe the signature of each layer. In these results, the most interesting feature is the upward inclination of the signature of the *horizontal* interface between the third layer and the basement of the model 2D. At first glance, this upward migration caused by the thickness enlargement of the upper layer looks suspicious. Nevertheless, if we analyze it more carefully it can be explained easily. Indeed, we know that the electromagnetic velocity in a lossless medium is given by $c/\sqrt{\varepsilon_r}$ where *c* is the velocity of light in the vacuum (0.3 m/ns) and ε_r is the relative permittivity of the medium. With this simple formula we can compute the zero offset arrival time as shown in Table II. The total time for the three layers at the left and right sides are respectively 123.96 and 114.70 ns, which are very closed to the values observed on Figure 4b.

TABLE II - Arrival times for layered earth models at the left and right sides of the model 2D.

Layer	ε_r	v (m/ns)	Left side		Right side	
			Twice the thickness (m)	Time (ns)	Twice the thickness (m)	Time (ns)
1	7	0.11339	4	35.28	4	35.28
2	5	0.13416	2	14.90	5	37.26
3	10	0.09487	7	73.78	4	42.16

In the second experiment we include the losses (see Table I). The first and second interfaces still can be clearly identified on the radargrams of Figure 5a and 5b. The lowermost interface, however, is no longer observed. In the third and last experiment we increased lightly the conductivities of the first and second layers (see Table II), therefore increasing the losses. We still can see the upper two layers in the model 1-D (Figure 6a). However in the model 2-D the left side (the deeper one) of the second interface is barely seen on the radargram of Figure 6b. As before, the lowermost interface is completely obscured.

CONCLUSIONS

Despite its simplicity and idealist conception, the algorithm it is very effective for forward modeling of two-dimensional GPR responses. Very complex two-dimensional earth can be easily analyzed because the flexibility of the finite element technique. Losses can be easily incorporated in the model. Magnetic permeability can also be included effortlessly. The next step is to use a more realistic antenna, for example, a finite length horizontal electric dipole. In this case the model is known as 2.5 dimensional and it will be much more involved computationally, of course.
.

REFERENCES

Schoolmeeters, J. W. A. V., Slob, E. C. and Fokkema, J. T., 1995, *Forward Modeling of Ground-Penetrating Radar Data for a Horizontal Layered Earth. Expanded Abstracts from 4th International Congress of the Brazilian Geophysical Society, Volume II, 939-941, Rio de Janeiro.*

Strang G. and Fix, G. J., 1973, *An Analysis of the Finite Element Method. Prentice-Hall, Englewood Cliffs, N. J.*

Wait, J. R., 1962, *Electromagnetic Waves in Stratified Media. Pergamon Press Book, New York*

ACKNOLEDGMENTS

This work was supported by CAPES and PADCT.

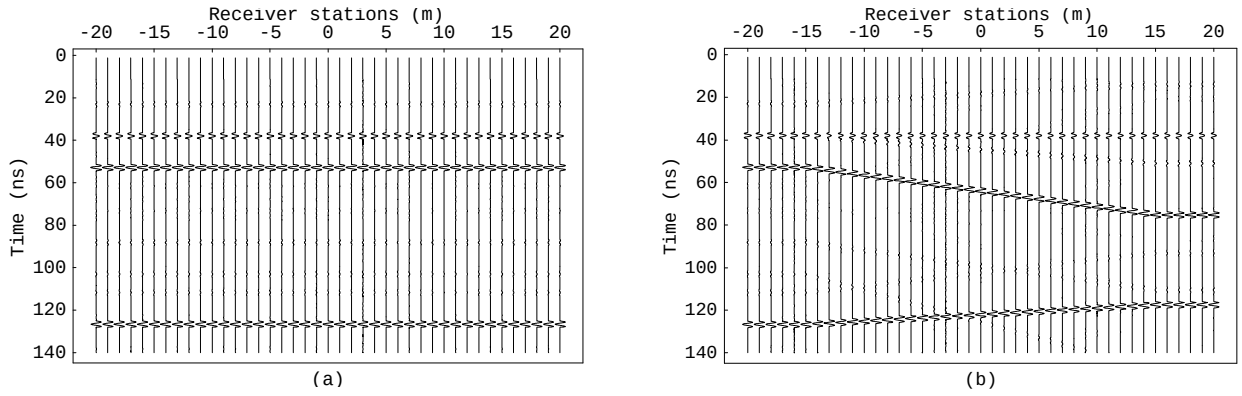

Figure. 4 Radargrams of Model 1-D (a) and Model 2-D (b), losses excluded ($\sigma_1 = \sigma_2 = \sigma_3 = \sigma_4 = 0$ S/m)

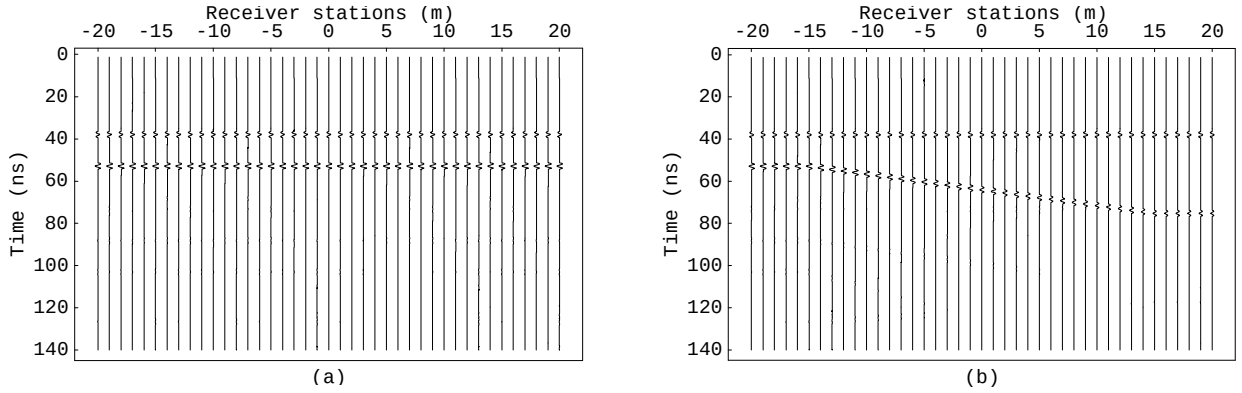

Figure. 5 Radargrams of Model 1-D (a) and Model 2-D (b), losses included ($\sigma_1 = 0.001$, $\sigma_2 = 0.002$, $\sigma_3 = 0.01$ and $\sigma_4 = 0.005$ S/m)

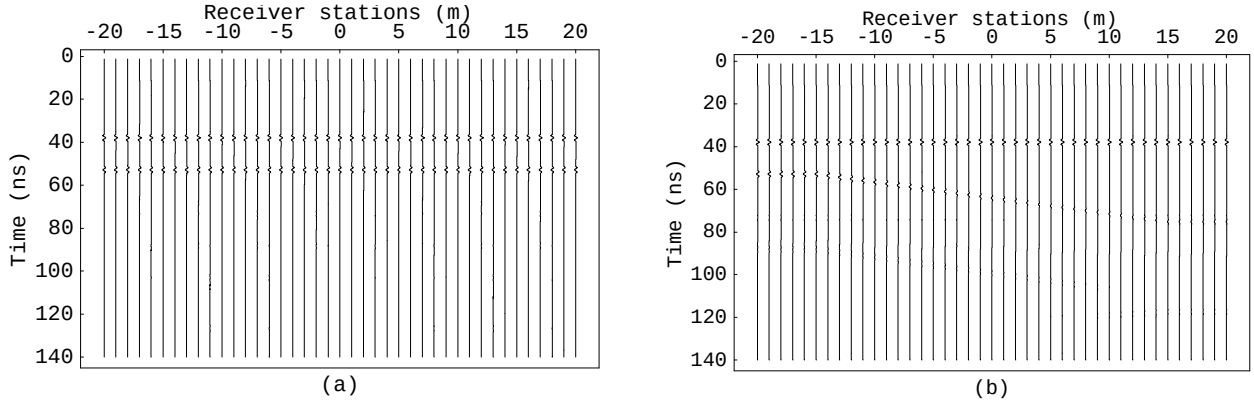

Figure. 6 Radargrams of Model 1-D (a) and Model 2-D (b), losses included ($\sigma_1 = 0.002$, $\sigma_2 = 0.005$, $\sigma_3 = 0.01$ and $\sigma_4 = 0.005$ S/m)